

Dynamic Pairing Effects on Low-Frequency Modes of Excitation in Deformed Mg Isotopes close to the Neutron Drip Line

Kenichi Yoshida¹, Masayuki Yamagami², and Kenichi Matsuyanagi¹

¹*Department of Physics, Graduate School of Science, Kyoto University, Kyoto 606-8502, Japan*

²*Heavy Ion Nuclear Physics Laboratory, RIKEN, Wako, Saitama 351-0198, Japan*

Low-frequency quadrupole vibrations in deformed $^{36,38,40}\text{Mg}$ are studied by means of the deformed Quasiparticle-RPA based on the coordinate-space Hartree-Fock-Bogoliubov formalism. Strongly collective $K^\pi = 0^+$ and 2^+ excitation modes (carrying 10-20 W.u.) are obtained at about 3 MeV. It is found that dynamical pairing effects play an essential role in generating these modes. It implies that the lowest $K^\pi = 0^+$ excitation modes are particularly sensitive indicators of dynamical pairing correlations in deformed nuclei near the neutron drip line.

PACS numbers: 21.60.Ev, 21.60.Jz, 21.10.Re

1. Introduction

The physics of drip-line nuclei is one of the current frontiers in nuclear structure physics. The number of unstable nuclei experimentally accessible will remarkably increase when the next generation of radioactive ion beam facilities start running, and we shall be able to study the properties not only of the ground states but also of low-lying excited states of drip-line nuclei in the medium-mass region. In order to quest for the new kinds of excitation mode unique to unstable nuclei associated with new features such as neutron skins, many attempts have been made using the self-consistent RPA based on the Skyrme-Hartree-Fock (SHF) method [1, 2] and the Quasiparticle RPA (QRPA) including the pair correlations [3, 4, 5, 6, 7]. Most of these calculations, however, are restricted to spherical nuclei, and low-frequency RPA modes in deformed unstable nuclei remain largely unexplored, except for some recent attempts [8, 9, 10].

In Ref. [11], we investigated properties of octupole excitations built on superdeformed states in neutron-rich sulfur isotopes by means of the RPA based on the deformed Woods-Saxon potential in the coordinate-mesh representation. We found that low-lying states created by excitation of a single neutron from a loosely bound low- Ω state to a high- Ω resonance state acquire extremely strong octupole transition strengths due to very extended spatial structure of particle-hole wave functions. We have extended this work to include pairing correlations self-consistently, and constructed a new computer code that carries out the deformed QRPA calculation on the basis of the coordinate-space Hartree-Fock-Bogoliubov (HFB) formalism [12]. In this paper, we report a new result of the deformed QRPA calculation for low-frequency soft quadrupole modes with $K^\pi = 0^+$ and 2^+ in $^{36,38,40}\text{Mg}$ close to the neutron drip line. According to the Skyrme-HFB calculations [13, 14], these isotopes are well deformed. The shell-model calculation [15] also suggests that the ground state of ^{40}Mg is dominated by the neutron $2p-2h$ components indicating breaking of the $N = 28$ shell closure. We have studied properties of soft modes of excitation in these Mg isotopes simultaneously taking into account the deformed mean-field effects, the pair-

ing correlations, and excitations to the continuum, and made microscopic analysis of the mechanism of generating these collective modes. The result of calculation suggests that the soft $K^\pi = 0^+$ modes are particularly sensitive indicators of dynamical pairing correlations in deformed nuclei near the neutron drip line.

2. Method

2.1. Mean-field calculation

Assuming axially symmetric deformation, we solve the HFB equation [12, 16],

$$\begin{pmatrix} h^q(\mathbf{r}\sigma) - \lambda & \tilde{h}^q(\mathbf{r}\sigma) \\ \tilde{h}^q(\mathbf{r}\sigma) & -(h^q(\mathbf{r}\sigma) - \lambda) \end{pmatrix} \begin{pmatrix} \varphi_{1,\alpha}^q(\mathbf{r}\sigma) \\ \varphi_{2,\alpha}^q(\mathbf{r}\sigma) \end{pmatrix} = E_\alpha \begin{pmatrix} \varphi_{1,\alpha}^q(\mathbf{r}\sigma) \\ \varphi_{2,\alpha}^q(\mathbf{r}\sigma) \end{pmatrix}, \quad (1)$$

on a two-dimensional lattice discretizing the cylindrical coordinates (ρ, z) . For the mean-field Hamiltonian h , we employ the deformed Woods-Saxon potential with the parameters used in [11] except for the isovector potential strength depending on the neutron excess, for which a slightly smaller value, 30 MeV, is adopted in order to describe ^{40}Mg as a drip-line nucleus in accordance with the Skyrme-HFB calculations [13, 14]. The pairing field \tilde{h} is treated self-consistently using the surface-type density-dependent contact interaction,

$$v_{pp}(\mathbf{r}, \mathbf{r}') = V_0 \left(1 - \frac{\varrho^{\text{IS}}(\mathbf{r})}{\varrho_0} \right) \delta(\mathbf{r} - \mathbf{r}'), \quad (2)$$

with $V_0 = -450 \text{ MeV}\cdot\text{fm}^3$ and $\varrho_0 = 0.16 \text{ fm}^{-3}$, where $\varrho^{\text{IS}}(\mathbf{r})$ denotes the isoscalar density. We use the lattice mesh size $\Delta\rho = \Delta z = 0.8 \text{ fm}$ and the box boundary condition at $\rho_{\text{max}} = 10.0 \text{ fm}$ and $z_{\text{max}} = 12.8 \text{ fm}$. The quasiparticle energy is cut off at 50 MeV.

2.2. Quasiparticle-RPA calculation

Using the quasiparticle basis obtained in the previous subsection, we solve the QRPA equation in the standard

matrix formulation,

$$\sum_{\gamma\delta} \begin{pmatrix} A_{\alpha\beta\gamma\delta} & B_{\alpha\beta\gamma\delta} \\ B_{\alpha\beta\gamma\delta}^* & A_{\alpha\beta\gamma\delta}^* \end{pmatrix} \begin{pmatrix} f_{\gamma\delta}^\lambda \\ g_{\gamma\delta}^\lambda \end{pmatrix} = \hbar\omega_\lambda \begin{pmatrix} 1 & 0 \\ 0 & -1 \end{pmatrix} \begin{pmatrix} f_{\alpha\beta}^\lambda \\ g_{\alpha\beta}^\lambda \end{pmatrix}. \quad (3)$$

For residual interactions, we use the Skyrme-type interaction for the particle-hole channel,

$$v_{ph}(\mathbf{r}, \mathbf{r}') = \left[t_0(1+x_0 P_\sigma) + \frac{t_3}{6}(1+x_3 P_\sigma) \varrho^{\text{IS}}(\mathbf{r}) \right] \delta(\mathbf{r} - \mathbf{r}'), \quad (4)$$

with $t_0 = -1100 \text{ MeV}\cdot\text{fm}^3$, $t_3 = 16000 \text{ MeV}\cdot\text{fm}^6$, $x_0 = 0.5$, $x_3 = 1.0$, P_σ being the spin exchange operator. The density-dependent contact interaction (2) is used for the particle-particle channel. Because the deformed Wood-Saxon potential is used for the mean-field, we renormalize the residual interaction in the particle-hole channel by multiplying a factor f_{ph} to get the spurious $K^\pi = 1^+$ mode (associated with the rotation) at zero energy ($v_{ph} \rightarrow f_{ph} \cdot v_{ph}$). We cut the model space for the QRPA calculation by $E_\alpha + E_\beta \leq 30 \text{ MeV}$ which is smaller than that for the HFB calculation. Accordingly, we need another self-consistency factor f_{pp} for the particle-particle channel. We determine this factor such that the spurious $K^\pi = 0^+$ modes (associated with the number fluctuation) appear at zero energy ($v_{pp} \rightarrow f_{pp} \cdot v_{pp}$).

The intrinsic matrix elements $\langle \lambda | Q_{2K} | 0 \rangle$ of the quadrupole operator Q_{2K} between the excited state $|\lambda\rangle$ and the ground state $|0\rangle$ are given by

$$\langle \lambda | Q_{2K} | 0 \rangle = \sum_{\alpha\beta} \left(Q_{2K}^{\alpha\beta} f_{\alpha\beta}^\lambda + Q_{2K}^{\beta\alpha} g_{\alpha\beta}^\lambda \right) = \sum_{\alpha\beta} M_{2K}^{\alpha\beta}, \quad (5)$$

where

$$Q_{2K}^{\alpha\beta} \equiv 2\pi \delta_{K,\Omega_\alpha+\Omega_\beta} \int d\rho dz Q_{2K}^{\alpha\beta}(\rho, z). \quad (6)$$

We calculate the intrinsic strength functions,

$$S^{\text{IS}}(\omega) = \sum_{\lambda} |\langle \lambda | Q_{2K}^{\text{IS}} | 0 \rangle|^2 \delta(\hbar\omega - \hbar\omega_{\lambda}), \quad (7)$$

for the isoscalar quadrupole operators Q_{2K}^{IS} , and use the notation $B(Q^{\text{IS}}2) = |\langle \lambda | Q_{2K}^{\text{IS}} | 0 \rangle|^2$.

3. Results and discussion

Calculated quadrupole transition strengths for the $K^\pi = 0^+$ and 2^+ excitations in $^{36,38,40}\text{Mg}$ are displayed in Fig. 1. We see prominent peaks at 2.9 and 3.3 MeV associated with the $K^\pi = 2^+$ and 0^+ modes, respectively, in ^{36}Mg ; at 2.8 MeV for the $K^\pi = 2^+$ mode in ^{38}Mg ; at 2.8 and 2.9 MeV for the $K^\pi = 2^+$ and 0^+ modes, respectively, in ^{40}Mg . This figure indicates that the transition strengths are very large (10-20 W.u.) and increase as we approach the neutron drip line. Figure 2 shows the ratios of the matrix elements for neutrons and protons. It is seen that the neutron excitation becomes dominant as the neutron number increases.

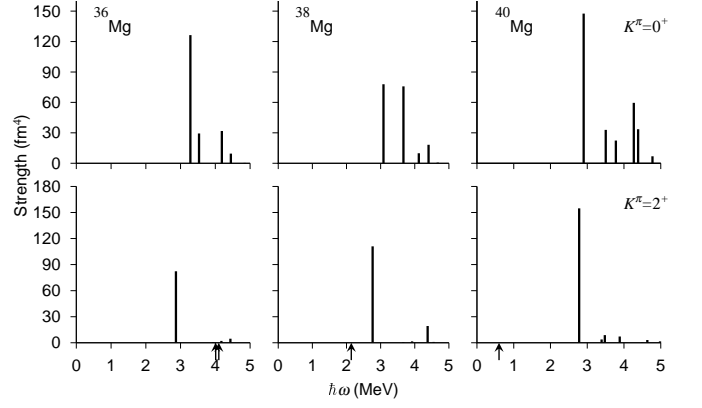


FIG. 1: Isoscalar quadrupole strengths $B(Q^{\text{IS}}2)$ for the $K = 0^+$ (upper panel) and $K = 2^+$ excitations (lower panel) on the prolate ground states of $^{36,38,40}\text{Mg}$, obtained by the deformed QRPA calculation with $\beta_2 = 0.28$. The arrows indicate the neutron threshold energy; $E_{\text{th}} = 4.01 \text{ MeV}$ (1qp continuum), 4.1 MeV (2qp continuum) for ^{36}Mg , 2.14 MeV for ^{38}Mg and 0.60 MeV for ^{40}Mg .

Let us focus our attention on the properties of excited states in ^{40}Mg . Details of the transition strength for the $K^\pi = 0^+$ excitations are displayed in Fig. 3. We immediately notice that the transition strength for the lowest excited state is significantly enhanced from that of the unperturbed two-quasiparticle excitations. From the QRPA amplitude listed in Table I, it is clear that this collective mode is generated by coherent superposition of neutron excitations of both particle-hole and particle-particle types. Let us discuss the reason why this mode acquires eminently large transition strength. In Ref. [11], we pointed out several examples where a neutron excitation from a loosely bound hole state to a resonant particle state brings about very large transition strength. This is a natural consequence of the fact that their wave functions are significantly extended from the nuclear surface. In the present calculation for ^{40}Mg , this effect is much enhanced due to the pairing correla-

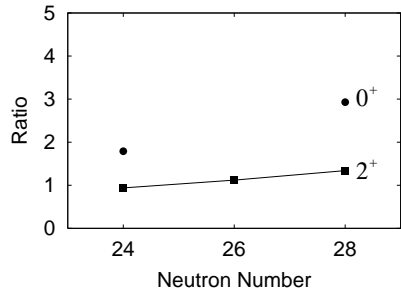


FIG. 2: Ratios of the neutron and proton matrix elements M_{ν}/M_{π} , divided by N/Z , are plotted as functions of neutron number. Filled circles and squares indicate the ratios for the lowest $K^\pi = 0^+$ and 2^+ modes, respectively.

TABLE I: QRPA amplitudes of the soft $K^\pi = 0^+$ mode at 2.9 MeV in ^{40}Mg . This mode has $B(E2) = 2.4 e^2\text{fm}^4$, $B(Q^\nu 2) = 112 \text{ fm}^4$, and $B(Q^{\text{IS}} 2) = 148 \text{ fm}^4$. The single-particle levels are labeled with the asymptotic quantum numbers $[Nn_3\Lambda]\Omega$ of the dominant components of the wave functions. Only components with $|f_{\alpha\beta}| > 0.1$ are listed.

	α	β	$E_\alpha + E_\beta$ (MeV)	$f_{\alpha\beta}$	$Q_{20}^{\alpha\beta}$ (fm 2)	$M_{20}^{\alpha\beta}$ (fm 2)
(a)	$\nu[310]1/2$	$\nu[310]1/2$	3.25	-0.633	5.55	-3.56
(b)	$\nu[312]3/2$	$\nu[312]3/2$	3.58	0.560	-2.04	-1.17
(c)	$\nu[301]1/2$	$\nu[310]1/2$	3.60	0.437	-3.08	-1.35
(d)	$\nu[301]1/2$	$\nu[301]1/2$	3.96	0.123	1.64	0.236
(e)	$\nu[303]7/2$	$\nu[303]7/2$	5.01	0.277	-3.34	-0.987
(f)	$\nu[321]3/2$	$\nu[321]3/2$	6.97	-0.124	3.08	-0.423

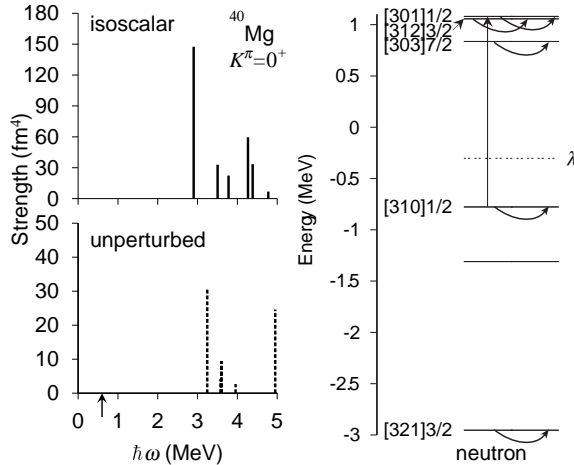


FIG. 3: *Left:* Isoscalar quadrupole strengths $B(Q^{\text{IS}} 2)$ for the $K^\pi = 0^+$ excitations in ^{40}Mg are plotted in the upper panel, while unperturbed two-quasiparticle strengths are shown in the lower panel. The arrow indicates the threshold energy $2|\lambda| = 0.60 \text{ MeV}$. *Right:* Two-quasiparticle excitations generating the soft $K^\pi = 0^+$ mode at 2.9 MeV. The pertinent levels are labeled with the asymptotic quantum numbers $[Nn_3\Lambda]\Omega$. The Fermi surface for neutrons is indicated by the dashed line.

tions among these loosely bound and resonance states. To show this point, we plot in Fig. 4 spatial distributions of two-quasiparticle wave functions generating the soft $K^\pi = 0^+$ mode. We see that these are significantly extended beyond the half-density radius. In addition, their spatial structures are rather similar; this is a favorable situation to generates coherence among them. In Fig. 5 we show how the transition strengths for the $K^\pi = 0^+$ and 2^+ modes change if the residual particle-particle interactions are ignored. We see that, although the prominent peak for the $K^\pi = 2^+$ mode still remains, the transition strength decreases. For the $K^\pi = 0^+$ mode, we notice a more striking effect; the prominent peak seen in Fig. 1 disappears when the dynamical pairing correlation is absent. Therefore we can say that the coherent superposition of particle-hole, particle-particle and hole-hole excitations is indispensable for the emergence

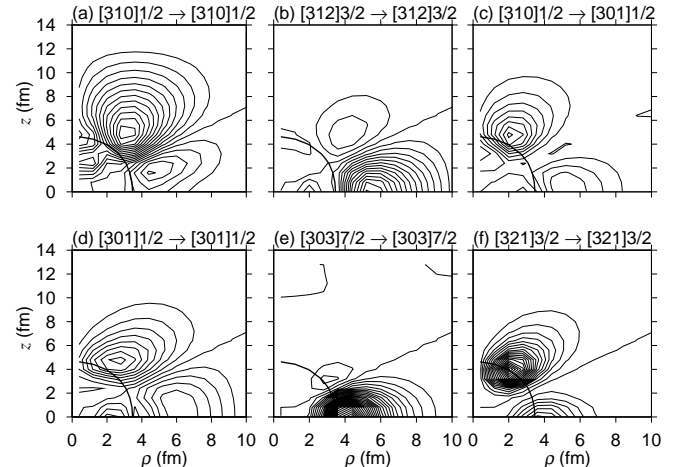


FIG. 4: Spatial distribution functions $Q_{20}^{\alpha\beta}(\rho, z)$ for some two-quasiparticle excitations generating the soft $K^\pi = 0^+$ mode in ^{40}Mg . The contour lines are plotted at intervals of 0.002. The thick solid line indicates the neutron half density radius.

of this mode. The importance of the coupling between the (particle-hole type) β vibration and the (particle-particle and hole-hole type) pairing vibration has been well known in stable deformed nuclei [17]. A new feature of the soft $K^\pi = 0^+$ mode in neutron drip-line nuclei is that this coupling takes place among two-quasiparticle excitations that are loosely bound or resonances, so that the transition strengths are extremely enhanced.

We examined the numerical stability of this soft $K^\pi = 0^+$ mode against variation of the box size. In Fig. 6 we show the isoscalar and unperturbed two-quasiparticle transition strengths for the $K^\pi = 0^+$ excitations in ^{40}Mg , obtained by using a larger box; $\rho_{\text{max}} \times z_{\text{max}} = 13.2 \text{ fm} \times 16.0 \text{ fm}$. We see that the position and the strength of the prominent peak are almost unchanged. This result confirms that the main two-quasiparticle components generating this mode are weakly bound and resonant states, and that the numerical error associated with the continuum discretization is not very significant.

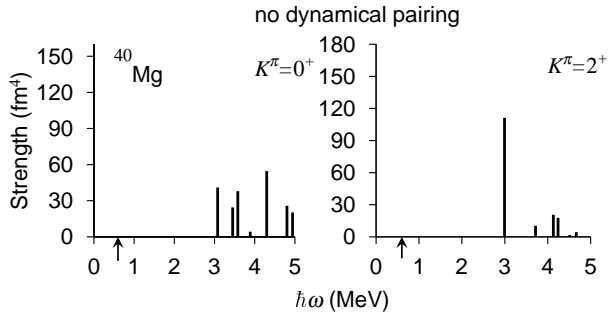


FIG. 5: Isoscalar quadrupole strengths for the $K^\pi = 0^+$ and 2^+ excitations in ^{40}Mg , obtained by switching off the residual particle-particle interactions.

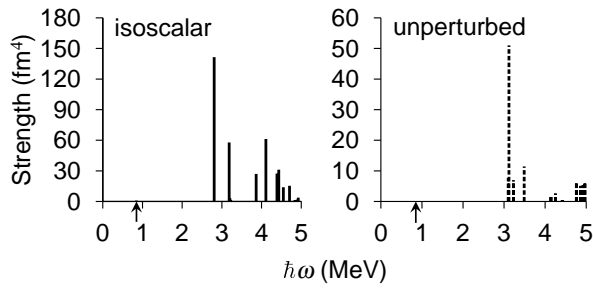


FIG. 6: *Left*: The isoscalar transition strengths for the $K^\pi = 0^+$ excitations in ^{40}Mg calculated using the box with size $\rho_{\text{max}} \times z_{\text{max}} = 13.2 \text{ fm} \times 16.0 \text{ fm}$. *Right*: Unperturbed two-quasiparticle strengths.

4. Conclusion

We have investigated properties of excitation modes in deformed Mg isotopes close to the neutron drip line by

means of the deformed QRPA based on the coordinate-space HFB. For $^{36,38,40}\text{Mg}$, we have obtained the soft $K^\pi = 0^+$ and 2^+ modes possessing large transition strengths. The microscopic mechanism of enhancement of the $K^\pi = 0^+$ strength is especially interesting. There are two causes for this enhancement; 1) the strong coupling occurs between the quadrupole shape vibration and the neutron pairing vibration, and 2) the two quasiparticle configurations coherently generating the $K^\pi = 0^+$ modes possess significantly extended spatial structures. The first cause has been well known in studies of stable deformed nuclei [17], but the second cause is unique to unstable deformed nuclei near the neutron drip line. The nature and roles of pair correlations for collective excitations in drip-line nuclei is currently under lively discussions [18]. On the basis of the deformed QRPA calculation demonstrating that the soft $K^\pi = 0^+$ mode is quite sensitive to the dynamical pairing, we suggest that an appearance of this soft mode is a very good indicator of pairing correlations in deformed drip-line nuclei.

Acknowledgments

This work was done as a part of the Japan-U.S. Cooperative Science Program “Mean-Field Approach to Collective Excitations in Unstable Medium-Mass and Heavy Nuclei”, and is supported by a Grant-in-Aid for the 21st Century COE “Center for Diversity and Universality in Physics” from the Ministry of Education, Culture, Sports, Science and Technology (MEXT) of Japan, and also by a Grant-in-Aid for Scientific Research No. 16540249 from the Japan Society for the Promotion of Science. The numerical calculations were performed on the NEC SX-5 supercomputer at Yukawa Institute for Theoretical Physics, Kyoto University.

[1] Hamamoto, I., Sagawa, H., and Zhang, X. Z., Phys. Rev. C **53**, 765 (1996); *ibid.* **64**, 024313 (2001).
[2] Shlomo, S and Agrawal, B., Nucl. Phys. A **722**, 98c (2003).
[3] Matsuo, M., Nucl. Phys. A **696**, 371 (2001).
[4] Hagino, K. and Sagawa, H., Nucl. Phys. A **695**, 82 (2001).
[5] Bender, M., Dobaczewski, J., Engel, J., and Nazarewicz, W., Phys. Rev. C **65**, 054322 (2002).
[6] Yamagami, M. and Van Giai, N., Phys. Rev. C **69**, 034301 (2004).
[7] Terasaki, J. *et al.*, Phys. Rev. C **71**, 034310 (2005).
[8] Urkedal, P., Zhang, X. Z., and Hamamoto, I., Phys. Rev. C **64**, 054304 (2001).
[9] Nakatsukasa, T. and Yabana, K., Phys. Rev. C **71**, 024301 (2005).
[10] Hagino, K., Van Giai, N. and Sagawa, H., Nucl. Phys. A **731**, 264 (2004).
[11] Yoshida, K., Yamagami, M. and Matsuyanagi, K., Prog. Theor. Phys. **116**, 1251 (2005).
[12] Dobaczewski, J., Flocard, H. and Treiner, J., Nucl. Phys. A **422**, 103 (1984).
[13] Terasaki, J., Flocard, H., Heenen, P.-H. and Bonche, P., Nucl. Phys. A **621**, 706 (1997).
[14] Stoitsov, M. V., Dobaczewski, J., Nazarewicz, W., Pittel, S., and Dean, D. J., Phys. Rev. C **68**, 054312 (2003).
[15] Caurier, E., Nowacki, F. and Poves, A., Nucl. Phys. A **742**, 14 (2004).
[16] Teran, E., Oberacker, V. E., and Umar, A. S., Phys. Rev. C **67**, 064314 (2003).
[17] Bohr, A., and Motteleson, B. R., “Nuclear Structure”, vol. II (Benjamin, 1975).
[18] Matsuo, M., Mizuyama, K., Serizawa, Y., Phys. Rev. C **71**, 064326 (2005).